

Cite this: *Dalton Trans.*, 2013, **42**, 1798

The formation of overlooked compounds in the reaction of methyl amine with the diethyl ester of *o*-phenylenebis(oxamic acid) in MeOH†

Mohammad A. Abdulmalic,^a Azar Aliabadi,^b Andreas Petr,^b Vladislav Kataev^b and Tobias Rüffer^{*a}

The treatment of the diethyl ester of *o*-phenylenebis(oxamic acid) (opbaH₂Et₂) with 2/3 of an equivalent of MeNH₂ in MeOH does not result in the formation of the methyl ester of *o*-phenylene(*N*'-methyloxamide)(oxamic acid) (opooH₃Me, **1**) in pure state, as reported previously. The colourless crude material formed by this reaction was confirmed to be composed of **1** (89% content), the dimethyl ester of *o*-phenylenebis(oxamic acid) (opbaH₂Me₂, **2**, 6%), 1,4-dihydro-2,3-quinoxalinedione (**3**, 3%) and *o*-phenylenebis(*N*'-methyloxamide) (opboH₄Me₂, **4**, 1%), respectively. The identities of **1–4** have been verified by IR, ¹H and ¹³C NMR spectroscopy as well as elemental analysis. In addition, the solid state structures of **1** and **2**·2DMSO, respectively, were determined by single-crystal X-ray diffraction studies. Successive recrystallization of the crude material from MeOH and MeOH : THF (1 : 1), respectively, does not give pure **1**, but a mixture of **1** and **2**. It is shown further that out of this mixture pure bis(oxamato) complexes cannot be obtained, as previously reported. Instead, treatment of the mixture with Ni^{II} or Cu^{II} salts, followed by the addition of [nBu₄N]OH, results in the formation of two mixtures of [nBu₄N]₂[Ni(opba)] (**5**) and [nBu₄N]₂[Ni(opooMe)] (**6**) as well as [nBu₄N]₂[Cu(opba)] (**7**) and [nBu₄N]₂[Cu(opooMe)] (**8**), respectively. The simultaneous formation of **5/6** and **7/8**, respectively, has been verified by crystallization of the obtained mixtures and X-ray diffraction studies of the obtained single crystals. Co-crystallization of mixtures of **5/6** (99 mass%) and **7/8** (1 mass%), respectively, results in the formation of single-crystals of diamagnetically diluted **7** in the host lattice of **5** (**7@5**) accompanied by single-crystal formation of diamagnetically diluted **8** in the host lattice of **6** (**8@6**), as verified by EPR spectroscopy. It is finally shown that the ethyl ester of *o*-phenylene(*N*'-methyloxamide)(oxamic acid) (opooH₃Et, **9**), a homologue of **1**, can be obtained in pure state by the treatment of opbaH₂Et₂ with 5/6 of an equivalent of MeNH₂ in EtOH.

Received 7th August 2012,
Accepted 25th October 2012

DOI: 10.1039/c2dt32259e

www.rsc.org/dalton

Introduction

o-Arylene or alkylene bis(oxamate or oxamide) derivatives represent versatile synthetic building blocks and have been broadly used as tetradentate ligands.¹ These compounds are able to coordinate metal ions *via* the N₂O₂ or N₄ donor sets to

form monometallic complexes.¹ Due to the flexidentate properties of these complexes, that is, to bind exogenous further metal ions *via* the *exo-cis* oxygen atoms, many kinds of bi- and trinuclear as well as polymeric complexes are achievable. These complexes are of manifold interest, for example, due to their supramolecular relevance or in the field of materials sciences.¹

Already in 1936, Gaade² synthesized diethyl-*N,N'*-ethylenebis(oxamate) as a first example of a starting material for the preparation of Cu^{II}-bis(oxamato) complexes. In general, the treatment of appropriate diamines with two equivalents of ethyloxalyl chloride or an excess of diethyl oxalate in the case of aliphatic diamines leads to diethyl-*N,N'*-diaminoalkylene- or arylene-bis(oxamates), of which a broad variety has been already synthesized.^{2–10}

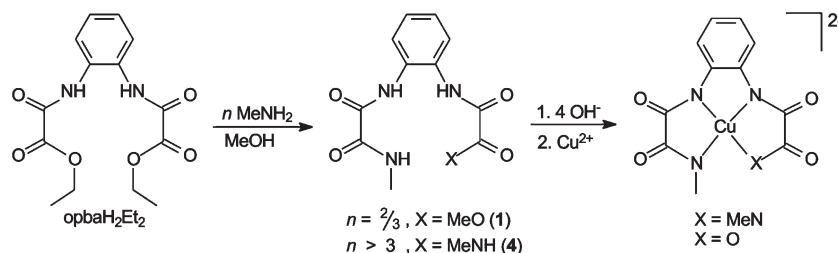
A survey of perhaps the simplest heteroatomsubstituted derivatives of diethyl-bis(oxamates), namely the bis(oxamides), in which the two O-Et groups are replaced by N(H)-R

^aTechnische Universität Chemnitz, Fakultät für Naturwissenschaften, Strasse der Nationen 62, D-09111 Chemnitz, Germany.

E-mail: tobias.rueffer@chemie.tu-chemnitz.de

^bLeibniz-Institut für Festkörper- und Werkstoffforschung IFW Dresden, PF 27 01 16, D-01171 Dresden, Germany

†Electronic supplementary information (ESI) available: Fig. S1–S15 give the ¹H, ¹³C NMR and IR spectra, respectively, of analyzed material and synthesized compounds. Fig. S16 gives an optical photograph of different kinds of single-crystals of diamagnetically diluted complexes. Transesterification reactions in the context of the investigated reaction are summarized in S17. CCDC 888732–888735. For ESI and crystallographic data in CIF or other electronic format see DOI: 10.1039/c2dt32259e



Scheme 1 Utilization of opbaH₂Et₂ for the synthesis of its derivatives **1** and **4** and their Cu^{II} complexes.^{11a}

(R = alkyl) groups, reveals astonishingly few reports.^{11,12} The synthesis of opboH₄Me₂ (**4**), obtained by the treatment of opbaH₂Et₂ with an excess of MeNH₂, was reported in 1997, *cf.* Scheme 1.^{11a} Out of the bis(oxamide) **4**, the corresponding Cu^{II} complex was synthesized and subsequently oxidized to its corresponding Cu^{III} complex.^{11a} The same report describes that the treatment of opbaH₂Et₂ with substoichiometric amounts of MeNH₂ in MeOH should result in the exclusive formation of opooH₃Me₂ (**1**), *cf.* Scheme 1. Starting from **1** in a supposed pure state, the synthesis of the corresponding Cu^{II} complexes in the form of Na⁺, Me₄N⁺ and PPh₄⁺ salts, respectively, is described as well.^{11a}

In our trials to synthesize [ⁿBu₄N]₂[M(opooMe)] (M = Ni (**6**), Cu (**8**)) using **1** prepared as described previously^{11a} and to obtain single-crystals of **8@6**, we were confronted with distinctive problems. These problems originate from impure **1** prepared according to the literature,^{11a} and commented in the following.

Results and discussion

Synthesis

The work undertaken in this report is a continuation of our recent research which dealt with the synthesis and EPR studies of [M(opooMe)]²⁺ (M = Ni^{II}, Cu^{II}) type complexes.¹³

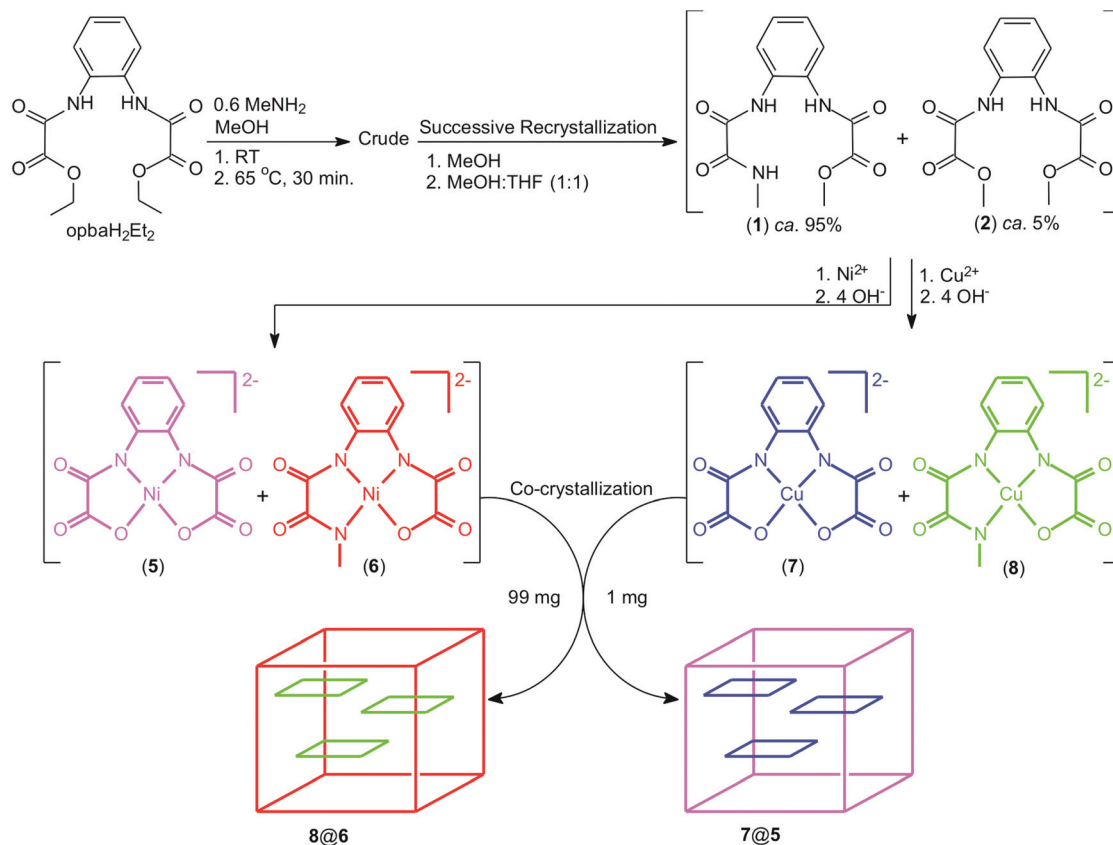
We repeated the synthesis of opooH₃Me₂ (**1**) first according to the procedure described in the literature and obtained in analogy a solid material.^{11a} That solid material is referred to in the following as “crude”. The elemental analysis data of the crude are in agreement with the values calculated for **1** and do not deviate significantly from the data given in the literature.^{11a} ¹H and ¹³C NMR spectra of the crude reveal, however, that **1** was not obtained in pure state. For pure **1**, for example, the ¹³C NMR should indicate the presence of up to ten distinguishable resonances originating from sp² hybridized carbon atoms, however, eighteen different resonances could be detected instead (Fig. S1†). Furthermore, for pure **1** three different N–H resonances with a ratio of 1 : 1 : 1 in the ¹H NMR are expected, whereas six different signals were detected instead (Fig. S1†).

In the report which describes the synthesis of proposed pure **1**, it is surprising to read that three different N–H resonances with a ratio of 1 : 2 : 2 are given.^{11a} The thus supposed pure **1** is then abbreviated as H₄L², where the number of

hydrogen atoms refers to N–H bonded ones.^{11a} The use of this abbreviation is incorrect. Furthermore, information given in the experimental part implies a yield of 90%, although opbaH₂Et₂ was treated with 2/3 of an equivalent of MeNH₂, which should result in a maximum yield of 66%.^{11a} The higher yield of **1** then implies the presence of further compounds in the isolated material taken for pure **1**.^{11a} This listing makes already clear that the synthesis of **1** reported so far in the literature^{11a,b} cannot give rise to pure **1** without additional effort. Our initial studies to access pure **1** and subsequent work with obtained materials are schematically illustrated in Scheme 2.

With the aim to obtain pure **1**, we recrystallized the obtained crude twice from MeOH and MeOH : THF (1 : 1), respectively, *cf.* Scheme 2. The elemental analysis data of the recrystallized material neither deviate significantly from those obtained for the crude nor supposed pure **1**. The ¹H and ¹³C NMR characterization of the recrystallized material reveals, however, that besides **1** one further compound is present, namely opbaH₂Me₂ (**2**), *cf.* Fig. S2.† The presence of **2** is concluded, for example, from its ¹H NMR chemical shifts at 3.87 ppm for the two O–CH₃ groups and at 10.40 ppm for the two N–H protons. Of course, ¹H NMR resonances of **2** do overlap with those of **1**, although from the ratio of the intensities of **2** compared to **1** the presence of *ca.* 5% of **2** and *ca.* 95% of **1** is concluded. Thus, even recrystallization of the crude does not give rise to pure **1**. Indeed, after inspecting the ¹H and ¹³C NMR spectra of the recrystallized material for the first time we were unaware of the presence of **2** and could not explain the origin of its NMR resonances. We thus started with the synthesis of the Ni^{II} and Cu^{II} complexes **6** and **8** of assumed pure **1**, *cf.* Scheme 2.

The recrystallized material obtained as described above was thus treated in MeOH with one equivalent of [Ni(OAc)₂(H₂O)₄] or half an equivalent of [Cu₂(OAc)₄(H₂O)₂]. Four equivalents of [ⁿBu₄N]OH were then added to the reaction mixtures. After appropriate workup, orange and purple coloured materials were isolated, respectively. The elemental analysis of the orange and purple coloured materials agrees with the formation of **6** and **8**, respectively. Afterwards, a mixture of 99 mass% of the orange material and 1 mass% of the purple coloured material was co-crystallized under diffusion controlled conditions from a combined MeCN solution against Et₂O with the aim to obtain **8@6**. Besides the formation of a small amount of well-shaped, orange coloured single-crystals, having clearly identifiable and addressable crystal faces required for orientation in EPR



Scheme 2 Synthesis of Ni^{II} and Cu^{II} complexes out of the recrystallized crude and the formation of 7@5 and 8@6 during co-crystallization.

experiments, a large amount of less well-shaped orange coloured single-crystals has been noticed.¹⁴

One of the well-shaped single crystals was selected for EPR measurements. Its typical EPR spectrum is shown in Fig. 1. The lines in the spectrum are grouped into four subsets due to the on-site hyperfine (HF) coupling of the Cu^{II} electron spin with its own nuclear spin. A clearly resolved structure of subsets arises due to the transferred HF coupling with the *N*-donor atoms. Considering the number of the lines in the subsets most likely only two *N*-donor atoms are coordinated to Cu^{II}. The *g*-factor of 2.074, a Cu hyperfine (HF) coupling constant of 116 G and a N HF-coupling constant of 16 G were obtained from modelling of the spectrum, *cf.* Fig. 1.

The obtained result of the EPR measurement verified that the well-shaped crystals represent 7@5, which was already studied by EPR measurements.¹⁵ One of the less well-shaped single crystals was then separated and studied by EPR. The results obtained thereof agree with the formation of 8@6 and are identical to those recently reported.¹³ The orange and purple coloured materials were then separately subjected to diffusion controlled crystallization from CH₂Cl₂, acetone and DMF solutions, respectively, against Et₂O.

For all performed crystallizations the orange and purple coloured materials gave rise to two even optically different kinds of single-crystals of pure 5 and pure 6, as well as pure 7 and pure 8, respectively.

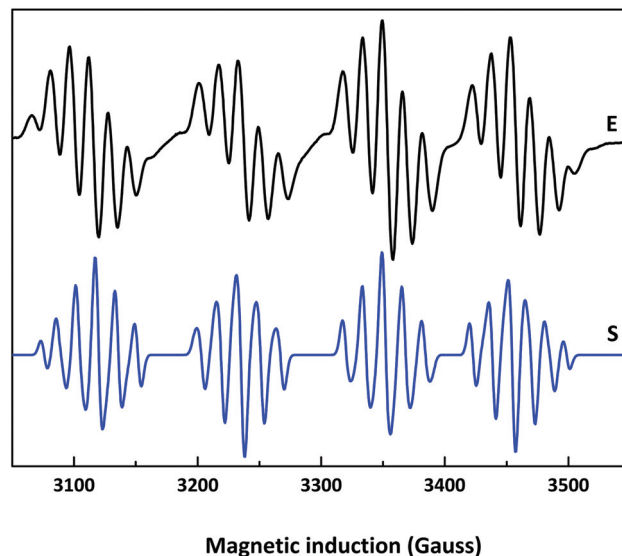


Fig. 1 Experimental (top) and simulated (bottom) EPR spectra of 7@5. The magnetic field was oriented at an angle of 50° with respect to the A₁₁ axis of the crystal to obtain the best resolved hyperfine patterns.

From the co-crystallization experiments we became aware that the recrystallized material is a mixture of 1 and 2. That prompted us to start with a resolution procedure of the

originally obtained crude material in order to identify its different components and to get access to pure **1**.

The separation process of the crude

The only satisfactory method of separation employed in order to isolate the different compounds forming the crude in their pure states was to use recurring Soxhlet-extractions under optimized conditions. The whole separation process, giving rise to the isolation of opbaH₂Me₂ (**2**), 1,4-dihydro-2,3-quinoxalinedione (**3**), opboH₄Me₂ (**4**) and finally opooH₃Me (**1**), respectively, in pure state is summarized in Scheme 3.

A first Soxhlet-extraction of the crude with THF for three hours (*ca.* 6 runs) was performed. After removal of all THF the obtained residue **A**, *cf.* Scheme 3, could be analyzed as pure opbaH₄Me₂ (**2**) in 6% yield based on the amount of the crude used (Fig. S3 and S4[†]). The THF-insoluble residue **B** was dried with a steam of argon. The NMR characterization indicates that residue **B** is free of **2** (Fig. S5[†]).

Residue **B** was then subjected to a Soxhlet-extraction with 100 mL of MeOH. This extraction did resolve nearly all residue **B**. After *ca.* seven hours extraction time the MeOH-insoluble material in the Soxhlet thimble, referred to as residue **D** (Scheme 3), was dried on air, recrystallized from MeOH:DMSO (2 : 1) and finally dried *in vacuo*. The characterization of residue **D** refers this material as pure 1,4-dihydro-2,3-quinoxalinedione (**3**) in 3% yield (Fig. S6 and S7[†]).

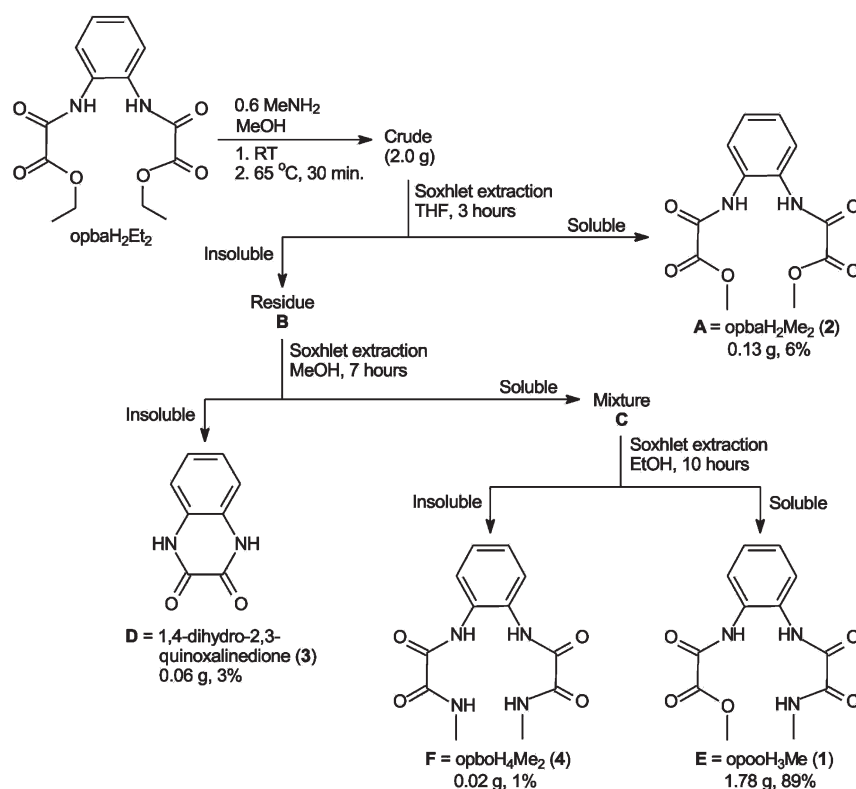
The MeOH solution, obtained from the Soxhlet-extraction of **B**, was evaporated to dryness. The obtained material is

referred to as residue **C**. The NMR characterization of residue **C** did reveal that this material is composed of two different compounds (Fig. S8[†]), one in major and the other in minor quantity. For example, in the ¹H NMR of **C** between *ca.* 9 to 11 ppm three resonances, attributed to N–H protons, with a ratio of intensities of 1 : 1 : 1 can be seen at 8.97, 10.33 and 10.57 ppm, whereas an additional resonance with minor intensity appears at 10.48 ppm.

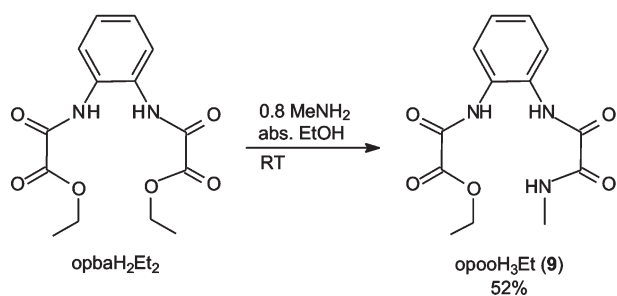
Residue **C** was thus subjected to a further Soxhlet-extraction with 100 mL EtOH for *ca.* 10 hours. After the collection of the EtOH-insoluble material, referred to as residue **F**, the characterization (Fig. S9 and S10[†]) reveals this material to be exclusively opboH₄Me₂ (**4**), in 1% yield. The EtOH extract **E** was evaporated to dryness to obtain a colourless solid. The characterization of **E** reveals now that the desired opooH₃Me₂ (**1**) is isolated in pure state in 89% yield (Fig. S11 and S12[†]).

Synthesis of the ethyl ester of *o*-phenylene(*N'*-methyloxamide) (oxamic acid) (opooH₃EtMe, **9**)

The isolation of pure **1** according to Scheme 3 is a very time consuming procedure. In order to have instant access to an asymmetric *N'*-alkyloxamide oxamic acid ester, several experiments were performed. It turned out that the treatment of opbaH₂Et₂ with 5/6 of an equivalent of MeNH₂ in absolute EtOH according to Scheme 4 is sufficient to gain **9** in *ca.* 50% yield in pure state (Fig. S13 and S14[†]).¹³ The comparatively low yield of **9** could indicate that besides **9** further compounds were formed. In order to check this, the following experiment



Scheme 3 Separation process to resolve the crude into its pure components **1–4**.



Scheme 4 Synthesis of opooH₃EtMe (**9**).

was performed: after the reaction had come to an end and the colourless solid formed was filtered off, the solvent of the filtrate was removed *in vacuo*. The NMR characterization of the obtained material revealed that besides a trace of **9** only unreacted opbaH₂Et₂ could be observed (Fig. S15[†]). That clearly indicates that the use of MeOH for the reaction of opbaH₂Et₂ with substoichiometric amounts of MeNH₂ is responsible for the formation of further products. The formation of **1** and **2** is clearly due to a transesterification reaction. The observation that **1** and **2** are formed comparatively quickly may open a new access to catalyzed transesterification reactions, *cf.* remarks given in S17.[†]

Structural descriptions

In order to prove the identities of the above separated compounds and complexes, especially of **1** and **2** and the complexes formed thereof, we tried to grow their single crystals suitable for X-ray diffraction studies. As mentioned above, single crystals of **5–8** have been obtained. In the following we report on the solid state structures of **1**, **2**, **5** and **7**, those of **6** and **8** have been recently reported.¹³

THE MOLECULAR AND CRYSTAL STRUCTURE OF OPOOH₃Me₂ (**1**). Single crystals of **1** have been obtained from DMSO:nitrobenzene (1:1) solutions of **1** layered by Et₂O. Compound **1** crystallizes in the non-centrosymmetric orthorhombic space group *Pna*2 (1). The absolute structure of **1** has been refined with respect to the Flack *x* parameter which is 0.0(5), whereas for the inverted structure a Flack *x* parameter of 0.8(5) is observed.¹⁶

Selected bond lengths, bond and torsion angles of **1** are given in Table 1, whereas Table 5 summarizes crystal and structural refinement data. The molecular structure of **1** is shown in Fig. 2 from two different perspective views. The chiral conformer of **1** observed in the solid state could be described as a planar chiral, with the chiral plane going through the C₆H₄N₂ fragment. As the oxamate unit possesses then a higher priority compared to the oxamate unit, the observed conformer can be described as *R_p*. Both the oxamate group (group I: N1, O1–O3, C1, C2, C11) and the oxaminate group (group II: N2, N3, O4, O5, C3, C4, C12) point to the same directions with respect to the central aromatic ring, *cf.* Fig. 2. Furthermore, the conformation of both groups I and II could be described as the *exo* (*anti*)-conformation. Both group I (root-mean-square deviation from planarity {rmsd in the following} = 0.0455 Å) and group II (rmsd = 0.0063 Å), respectively, are nearly planar. The interplanar angle between both groups amounts to 81.6(1)°. With respect to the central aromatic ring (C5–C10), group I is rotated by 55.4(°) and group II by 43.9(2)°.

No intramolecular hydrogen bonds between group I and group II are observed, *cf.* Fig. 2. This observation is in contrast to the finding for the related opbaH₂Et₂, where both oxamate groups interact by an intramolecular hydrogen bond.¹⁷ However, as observed for opbaH₂Et₂,¹⁷ compound **1** forms 1D chains along the crystallographic *c*-axes in the solid state due to intermolecular hydrogen bonds. A selected part of one 1D chain is shown in Fig. 3 together with a graphical illustration of the orientation of the 1D chains to each other and with respect to the unit cell. Data of the intermolecular hydrogen bonds are summarized in Table 2. As shown in Fig. 3, interacting molecules of **1** are parallel displaced superimposed with respect to each other and the interactions between all molecules of **1** within a 1D chain are always achieved by intermolecular hydrogen bonds of the type N–H...O. The 1D chains of opbaH₂Et₂, however, are formed by dimeric units of opbaH₂Et₂ with N–H...O type hydrogen bonds which are connected further to zigzag chains by means of C–H...O hydrogen bonds. This structural difference might show and underline that slight changes of the nature of a supramolecular synthon have fundamental impact on the supramolecular arrangement.

THE MOLECULAR AND CRYSTAL STRUCTURE OF OPBAH₂Me₂·2DMSO (**2**·2DMSO). Single crystals of **2** have been obtained from

Table 1 Selected bond lengths (Å), bond and torsion angles (°) of **1**

Bond lengths				Bond angles			
C1–N1	1.340(6)	C3–N2	1.340(6)	O1–C1–N1	127.1(5)	O4–C3–N4	126.2(5)
C1–O1	1.211(6)	C3–O4	1.248(6)	O1–C1–C2	121.6(4)	O4–C3–C4	119.7(4)
C1–C2	1.544(7)	C3–C4	1.543(7)	N1–C1–C2	111.3(5)	N2–C3–C4	114.1(4)
C2–O2	1.216(6)	C4–O5	1.236(6)	O3–C2–O2	125.7(5)	O5–C4–N3	126.2(5)
C2–O3	1.308(6)	C4–N3	1.303(7)	O3–C2–C1	112.2(5)	O5–C4–C3	119.6(4)
C5–N1	1.417(6)	C10–N2	1.425(6)	O2–C2–C1	122.1(4)	N3–C4–C3	114.2(4)
C5–C10	1.413(7)			C1–N1–C5	123.8(4)	C3–N2–C10	124.1(5)
Torsion angles				C1–N1–H1N	118(4)	C3–N2–H2N	121(3)
O1–C1–C2–O3	−6.7(7)	O4–C3–C4–N3	0.9(7)	C5–N1–H1N	118(4)	C10–N2–H2N	115(3)
N1–C1–C2–O3	174.5(4)	N2–C3–C4–N3	179.8(4)				
O1–C1–C2–O2	174.9(6)	O4–C3–C4–O5	0.1(5)				
N1–C1–C2–O2	−3.9(7)	N2–C3–C4–O5	−1.1(6)				

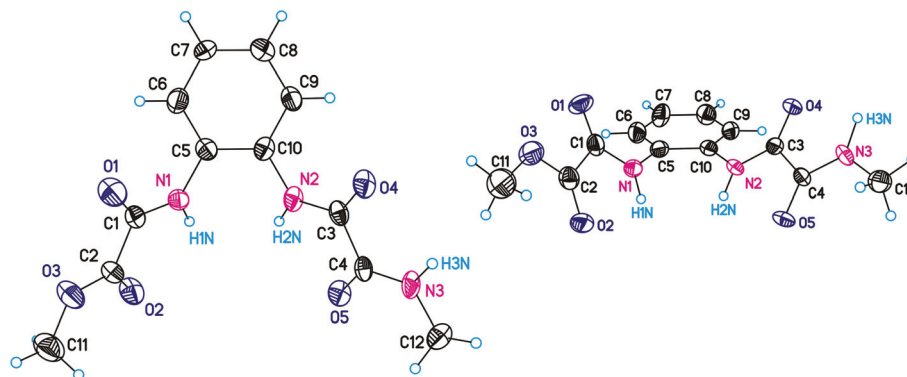


Fig. 2 ORTEP diagrams (50% ellipsoid probability) of the molecular structure of **1**. Left: top view. Right: side view.

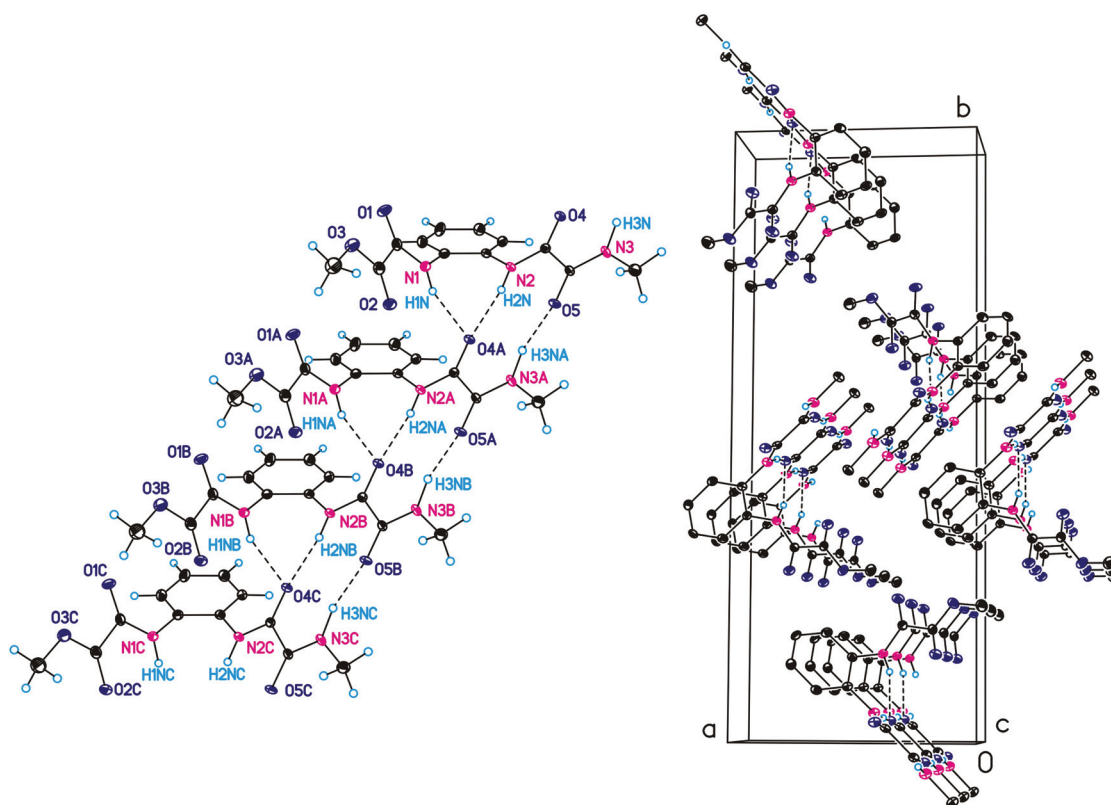


Fig. 3 Left: graphical representation of a selected part of a 1D chain formed by **1** in the solid state due to intermolecular hydrogen bonds. Label 'A' to 'C' refers to a first to the third symmetry generated molecule of **1**. Right: graphical representation of the orientation of the 1D chains formed by **1** along the crystallographic *c*-axis. All C-bonded hydrogen atoms are omitted for clarity.

Table 2 Selected bond lengths (Å) and angles (°) of the intermolecular hydrogen bonds of **1**

D-H...A	D-H	H...A	D...A	D-H...A
N1-H1N...O4A	0.92(7)	1.99(8)	2.850(6)	154(6)
N2-H2N...O4A	0.91(3)	1.96(3)	2.827(6)	162(3)
N3-H3N...O5A	1.06(6)	1.82(6)	2.856(6)	165(5)

Symmetry code 'A': $x, y, 1 + z$.

DMSO : CHCl₃ (1 : 9) solutions of **2** layered by "hexane. Compound **2** crystallizes in the centrosymmetric monoclinic space group *C2/c* in the form of a DMSO adduct as 2·2DMSO. Selected bond lengths, bond and torsion angles of 2·2DMSO are given in Table 3, whereas Table 5 summarizes crystal and structural refinement data. The molecular structure of 2·2DMSO is shown in Fig. 4 together with those of the opbaH₂Me₂ fragment, which is denoted in the following as **2A**. Compound 2·2DMSO possesses crystallographically imposed

C_2 symmetry. The interaction of the two DMSO molecules originates from hydrogen bonds between the N–H protons of **2A** and the oxygen atoms of DMSO, cf. Fig. 4. The donor...acceptor distance $N1\cdots O4$ amounts to 2.8777(17) Å and the $N1-H1N\cdots O4$ angle to 162.8(17)°. The interactions of the DMSO molecules rule out any possible formation of intermolecular hydrogen bonds and/or π interactions between molecules of **2**. The two oxamate groups of **2A** adopt the same conformation in the solid state, which could be described as an *exo(anti)*-conformation, although these groups point to opposite directions with respect to the plane of the aromatic ring. For the closely related $opbaH_2Et_2$ the two oxamate groups adopt different conformations, namely an *endo(anti)*- and an *exo(syn)*-conformation,¹⁷ although in the case of this compound no cocrystallization of any solvent molecule is observed.

The crystallographically independent oxamate group of **2A** is not planar, as the $O=C-OMe$ unit ($O2, O3, C2, C6$; rmsd =

0.0091 Å) is rotated by 19.7(3)° with respect to the $N(H)-C=O$ unit ($N1, H1N, C1, O1$; rmsd = 0.0199 Å). The *non*-planarity of the oxamate group is expressed in addition by the torsion angles given in Table 4 with, for example, the value for $N1-C1-C2-O2$ with 19.3(2)°. The $N(H)-C=O$ unit of **2A** is furthermore rotated by 44.7(2)° with respect to the C_6H_4 aromatic ring. All other structural features of **2A** agree very well with the corresponding data given for $opbaH_2Et_2$.¹⁷

THE MOLECULAR STRUCTURES OF $[^nBu_4N]_2[M(OPBA)]$ ($M = Ni$ (**5**), Cu (**7**)). Complexes **5** and **7** crystallize in the centrosymmetric monoclinic space group $C2/c$. Both complexes are isomorphic to each other, as related unit cell parameters are only slightly different. Selected bond lengths, bond and torsion angles of **5** and **7** are given in Table 4, whereas Table 5 summarizes crystal and structural refinement data of **5** and **7**.

The crystal structure of **5** and **7** consists of discrete $[^nBu_4N]^+$ cations and $[M(opba)]^{2-}$ anions, respectively. The anionic entities $[Ni(opba)]^{2-}$ (**5A**) and $[Cu(opba)]^{2-}$ (**7A**), respectively, possess crystallographically imposed C_2 symmetry and are both not perfectly planar as indicated in Fig. 5. Accordingly, the MO_2N_2 coordination setups are not strictly planar and the largest deviations are observed for the N atoms (**5A**: 0.0459(9) Å; **7A**: 0.0713(14) Å). The M atoms are otherwise precisely in the plane of calculated mean planes of their surrounding O_2N_2 donor atom setups. The M–N bond lengths of the MO_2N_2 coordination units of **5A** and **7A** are significantly shorter compared to the M–O bond lengths (**5A**: $Ni1-N1 = 1.8338(13)$ Å vs. $Ni1-O2 = 1.8933(12)$ Å; **7A**: $Cu1-N1 = 1.910(2)$ Å vs. $Cu1-O2 = 1.9428(19)$ Å).

There are already reports of complexes with discrete $[Ni(opba)]^{2-}$ complex fragments, namely $[Ni(meso-cth)][Ni(opba)] \cdot 2H_2O$ (**10**) (*meso-cth* = *meso*-5,7,7,12,14,14-hexamethyl-1,4,8,11-tetraazacyclotetradecane),¹⁸ and of complexes with discrete $[Cu(opba)]^{2-}$ complex fragments, namely $[Ni(meso-cth)][Cu(opba)] \cdot 2H_2O$ (**11**),¹⁹ $[PPh_4]_2[Cu(opba)]$ (**12**),²⁰ and $[Ru-$

Table 3 Selected bond lengths (Å), bond and torsion angles (°) of **2**·DMSO

Bond lengths		Bond angles	
C1–N1	1.3463(18)	O1–C1–N1	126.16(15)
C1–O1	1.2188(17)	O1–C1–C2	121.68(13)
C1–C2	1.531(2)	N1–C1–C2	112.16(13)
C2–O2	1.2023(18)	O3–C2–O2	125.45(15)
C2–O3	1.3287(17)	O3–C2–C1	110.30(13)
C3–N1	1.416(2)	O2–C2–C1	124.24(13)
C3–C3A ^a	1.406(3)	C1–N1–C3	123.02(13)
S1–O4	1.5084(12)	C1–N1–H1N	118.3(11)
Torsion angles		C3–N1–H1N	117.1(11)
O1–C1–C2–O3	18.11(19)		
N1–C1–C2–O3	–161.83(12)		
O1–C1–C2–O2	–160.79(15)		
N1–C1–C2–O2	19.3(2)		

^a Symmetry operation used to generate equivalent atoms 'A': $-x, y, -z - 1/2$.

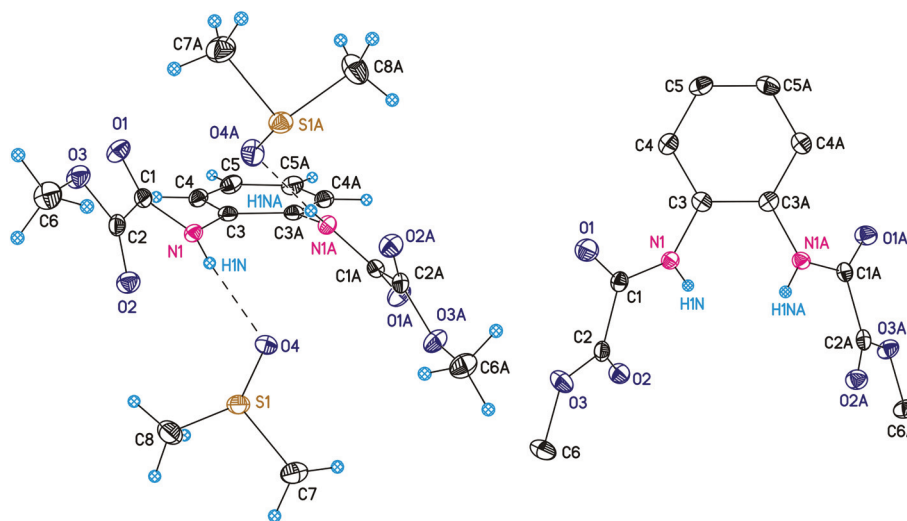


Fig. 4 ORTEP diagrams (50% ellipsoid probability, respectively) of the molecular structure of **2**·DMSO (left, side view) and of **2A** (right, top view, C-bonded hydrogen atoms are omitted for clarity). Symmetry operation used to generate equivalent atoms 'A': $-x, y, -z - 1/2$.

Table 4 Selected bond lengths (Å), bond and torsion angles (°) of **5A** and **7A**

Bond lengths	5A ^a	7A ^b	Bond angles	5A ^a	7A ^b
N1–M1	1.8338(13)	1.910(2)	N1–M1–N1A ^c	85.79(8)	84.19(13)
O2–M1	1.8933(12)	1.9428(19)	N1–M1–O2	86.18(5)	84.87(9)
C1–N1	1.332(2)	1.326(4)	N1A–M1–O2	171.49(6)	168.24(9)
C1–O1	1.246(2)	1.242(3)	O2–M1–O2A ^c	101.97(7)	106.34(11)
C1–C2	1.552(2)	1.558(4)	O1–C1–N1	128.59(16)	128.5(3)
C2–O2	1.294(2)	1.295(3)	O1–C1–C2	122.07(14)	121.1(2)
C2–O3	1.232(2)	1.235(3)	N1–C1–C2	109.35(14)	110.4(2)
C3–N1	1.406(2)	1.396(3)	O3–C2–O2	124.74(16)	124.6(3)
C3–C3A ^c	1.422(3)	1.430(6)	O3–C2–C1	120.02(15)	119.0(3)
Torsion angles			O2–C2–C1	115.24(14)	116.5(2)
O1–C1–C2–O3	1.2(2)	−0.2(3)	C1–N1–C3	128.83(14)	130.2(2)
N1–C1–C2–O3	−179.48(14)	179.4(2)	C1–N1–M1	116.58(11)	115.79(18)
O1–C1–C2–O2	−179.51(13)	179.3(2)	C3–N1–M1	114.59(10)	113.97(18)
N1–C1–C2–O2	−0.16(18)	−1.0(3)	C2–O2–M1	112.61(11)	112.34(17)

^a M1 = Ni1. ^b M1 = Cu1. ^c Symmetry operation used to generate equivalent atoms 'A'. **5A**: $-x + 2, y, -z + 3/2$. **7A**: $-x + 1, y, -z + 5/2$.

Table 5 Crystal and structural refinement data of **1**, **2**-DMSO, **5** and **7**

	1	2 -DMSO	5	7
Chemical formula	C ₁₂ H ₁₃ N ₃ O ₅	C ₁₆ H ₂₄ N ₂ O ₈ S ₂	C ₄₂ H ₇₆ N ₄ NiO ₆	C ₄₂ H ₇₆ CuN ₄ O ₆
Formula weight (g mol ^{−1})	279.25	436.49	791.78	796.61
Crystal system	Orthorhombic	Monoclinic	Monoclinic	Monoclinic
Space group	<i>Pna</i> 2(1)	<i>C2/c</i>	<i>C2/c</i>	<i>C2/c</i>
Unit cell dimensions (Å, °)	<i>a</i> = 10.1175(11) <i>b</i> = 25.335(3) <i>c</i> = 5.0430(4) α = 90.0 β = 90.0 γ = 90.0	15.3163(5) 9.0186(3) 14.8471(5) 90.0 98.034(4) 90.0	<i>a</i> = 18.5088(4) <i>b</i> = 17.1731(4) <i>c</i> = 14.2230(4) α = 90.0 β = 91.997(3) γ = 90.0	18.5716(9) 17.2023(7) 14.1556(5) 90.0 91.897(4) 9.0
Volume (Å ³)	1292.7(2)	2030.72(12)	4518.08(19)	4519.9(3)
Measurement temperature (K)	100	100	115	115
Radiation source	Cu K α	Mo K α	Cu K α	Cu K α
Wavelengths (Å)	1.54184	0.71073	1.54184	1.54184
<i>Z</i>	4	4	4	4
Density (calculated) (Mg m ^{−3})	1.435	1.428	1.164	1.171
Absorption coefficient (mm ^{−1})	0.967	0.308	0.983	1.045
<i>F</i> (000)	584	920	1728	1732
Reflections collected	4032	3450	7198	6968
Independent reflections/ <i>R</i> _{int} ^a	1633, 0.0618	1790, 0.0188	3542, 0.0204	3440, 0.0333
Index ranges	−11 ≤ <i>h</i> ≤ 11, −28 ≤ <i>k</i> ≤ 24, −5 ≤ <i>l</i> ≤ 4	−18 ≤ <i>h</i> ≤ 18, −10 ≤ <i>k</i> ≤ 10, −17 ≤ <i>l</i> ≤ 12	−21 ≤ <i>h</i> ≤ 21, −19 ≤ <i>k</i> ≤ 19, −11 ≤ <i>l</i> ≤ 16	−21 ≤ <i>h</i> ≤ 21, −16 ≤ <i>k</i> ≤ 19, −16 ≤ <i>l</i> ≤ 7
θ range for data collection (°)	3.49 to 63.07	3.58 to 25.05	3.51 to 62.71	4.64 to 62.76
Data/restraints/parameters	1633/2/193	1790/0/131	3542/0/240	3440/0/240
Goodness-of-fit on <i>F</i> ² ^b	0.953	1.0062	1.005	0.943
Final <i>R</i> indices [<i>I</i> > 2 σ (<i>I</i>)] ^c	<i>R</i> ₁ = 0.0598, <i>wR</i> ₂ = 0.1448	<i>R</i> ₁ = 0.0290, <i>wR</i> ₂ = 0.0703	<i>R</i> ₁ = 0.0391, <i>wR</i> ₂ = 0.1042	<i>R</i> ₁ = 0.0496, <i>wR</i> ₂ = 0.1246
<i>R</i> indices (all data) ^c	<i>R</i> ₁ = 0.0752, <i>wR</i> ₂ = 0.1521	<i>R</i> ₁ = 0.0357, <i>wR</i> ₂ = 0.0720	<i>R</i> ₁ = 0.0445, <i>wR</i> ₂ = 0.1069	<i>R</i> ₁ = 0.0639, <i>wR</i> ₂ = 0.1300
Flack <i>x</i> parameter ¹⁶	0.0(5)	—	—	—
Largest diff. peak/hole (e Å ^{−3})	0.313, −0.300	0.236, −0.302	0.407, −0.387	0.594, −0.310
Average/maximum shift/error	0.002/0.000	0.000/0.000	0.000/0.000	0.000/0.000

^a $R_{\text{int}} = \sum |F_o|^2 - F_o^2(\text{mean}) / \sum F_o^2$, where $F_o^2(\text{mean})$ is the average intensity of symmetry equivalent diffractions. ^b $S = [\sum (w(F_o^2 - F_c^2)^2) / (n - p)]^{1/2}$, where n = number of reflections, p = number of parameters. ^c $R = [\sum (|F_o| - |F_c|) / \sum |F_o|]$; $wR = [\sum (w(F_o^2 - F_c^2)^2) / \sum (wF_o^4)]^{1/2}$.

(bpy)₃] [Cu(opba)]·9H₂O (**13**).²¹ The observation that the M–N bonds of **5A** and **7A** are shorter compared to the M–O bonds is due to the greater basicity of the N (amide) compared to the O (carboxylate) donor atoms,²⁰ and has been observed for **10–13** as well.^{18–21} The Ni–N and Ni–O bond lengths of **5A** are significantly shorter compared to the related bond lengths of **7A** which reflects nicely the shorter ionic radius of Ni^{II} ions in a planar coordination environment compared to Cu^{II} ions (Ni^{II}: 63 pm vs. Cu^{II}: 71 pm).²² The same tendency is observed

when comparing related bond lengths of **10** with those of **11–13**.^{18–21}

Experimental part

All chemicals were purchased from commercial sources and used as received without further purification. The solvents were purified according to standard procedures.²³ NMR

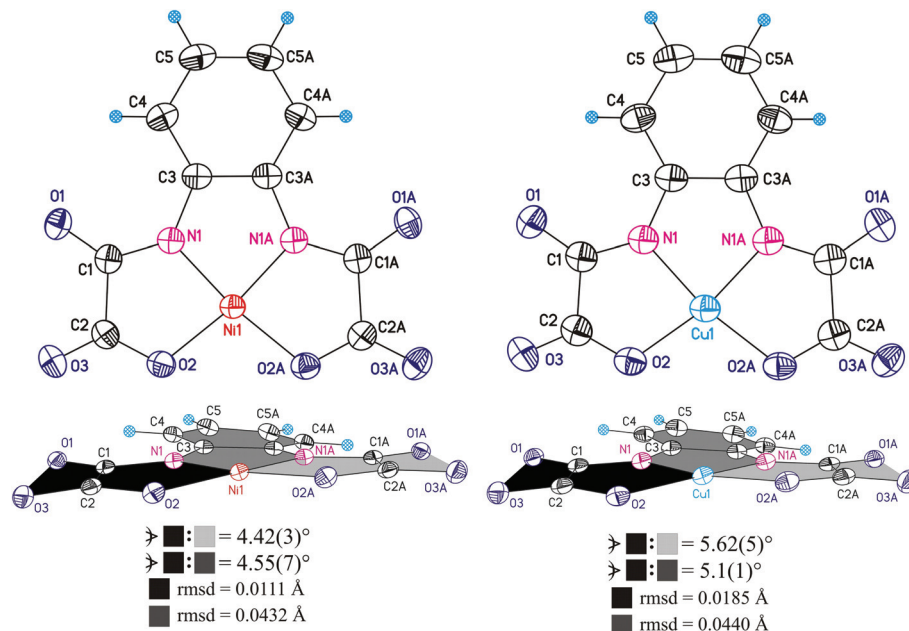


Fig. 5 ORTEP diagrams (50% ellipsoid probability) of the molecular structures of **5A** (left) and **7A** (right). Above: top view. Below: side view. Sign \angle refers to the interplanar angle and rmsd to the root-mean-square deviation from planarity of calculated mean planes of atoms adjoining differently coloured areas. Symmetry operation used to generate equivalent atoms 'A' **5A**: $-x + 2, y, -z + 3/2$. **7A**: $-x + 1, y, -z + 5/2$.

spectra were recorded at room temperature with a Bruker Avance III 500 UltraShield spectrometer (^1H at 500.300 MHz and $^{13}\text{C}\{^1\text{H}\}$ at 125.813 MHz) in the Fourier transform mode. Chemical shifts are reported in δ (ppm) vs. SiMe_4 with the solvent as the reference signal ($[\text{D}_6]\text{-DMSO}$: ^1H NMR, $\delta = 2.54$; and $^{13}\text{C}\{^1\text{H}\}$ NMR, $\delta = 40.45$). FT-IR spectra were recorded in the range of 400–4000 cm^{-1} on a Thermo Scientific Smart iTR spectrophotometer. Elemental analyses for C, H and N were performed using a Thermo FlashAE 1112 series. The diethyl ester of *N,N'*-*o*-phenylene-bis(oxamic acid) ($\text{opbaH}_2\text{Et}_2$) was synthesized according to a published procedure.⁴ EPR spectroscopy was done with an X-band spectrometer EMX (Bruker) at ambient temperature. The angular dependent measurements were done using a H_{103} cavity equipped with a goniometer.

Repeated reaction of $\text{opbaH}_2\text{Et}_2$ with MeNH_2 according to [11a]

A solution of $\text{opbaH}_2\text{Et}_2$ (0.01 mol, 3.08 g) in MeOH (50 mL) was treated with MeNH_2 (0.56 g, 0.0066 mol, 33% in EtOH) at room temperature. The mixture was kept at 65 °C for half an hour with vigorous stirring and the white precipitate was filtered off, washed with MeOH and Et_2O , and dried under vacuum. That material is referred to in the following as crude. Yield of crude: 1.53 g. Fig. S1† gives the ^1H and ^{13}C NMR as well as the IR spectra of the crude. Elemental analysis of the crude: anal. calcd (%) for $\text{C}_{12}\text{H}_{13}\text{N}_3\text{O}_5$ (279.25 g mol^{-1}): C 51.61, H 4.69, N 15.05; found: C 51.62, H 4.65, N 14.70.

The crude (ca. 3 g) was recrystallized twice from MeOH and MeOH:THF (1:1), respectively. Yield of recrystallized

material: 1.71 g. The ^1H and ^{13}C NMR spectra of the recrystallized material are given in Fig. S2.† The elemental analysis of the recrystallized material does not deviate significantly from the values obtained from the crude. According to the analytical characterization of the recrystallized material it is composed of the methyl ester of *o*-phenylene(*N'*-methyloxamide)(oxamic acid) ($\text{opooH}_3\text{Me}_2$, **1**) to ca. 95% content and the dimethyl ester of *o*-phenylenebis(oxamic acid) ($\text{opbaH}_2\text{Me}_2$, **2**) to ca. 5% content.

Synthesis and characterization of Cu^{II} and Ni^{II} complexes by using the recrystallized material obtained from the reaction of $\text{opbaH}_2\text{Et}_2$ and MeNH_2 in MeOH

The recrystallized material has been obtained as described above and is composed of $\text{opooH}_3\text{Me}_2$ (**1**, ca. 95%) and $\text{opbaH}_2\text{Me}_2$ (**2**, ca. 5%). In the following descriptions the used masses of the recrystallized material are given. The given molar amounts refer to assumption that this material is pure **1**.

Ni^{II} COMPLEXES. A hot solution (ca. 50 °C) of $[\text{Ni}(\text{OAc})_2(\text{H}_2\text{O})_4]$ (0.49 g, 0.002 mol) in MeOH (50 mL) was added dropwise with stirring to a hot suspension (ca. 50 °C) of the recrystallized material (0.55 g, 0.002 mol) in MeOH (50 mL). Then, $[\text{Bu}_4\text{N}]\text{-OH}$ (5.18 g, 40% in MeOH, 0.008 mol) was added with continuous stirring. The resulting mixture was stirred at 60 °C for a further 15 minutes, filtered and the solvent evaporated to dryness. The resulting oily material was treated with THF (25 mL) and filtered to eliminate $[\text{Bu}_4\text{N}]\text{OAc}$. The solid material was precipitated by addition of Et_2O (200 mL) as an orange powder, filtered and dried *in vacuo*. Yield: 1.07 g (66%).

Anal. calcd (%) for $C_{43}H_{79}NiN_5O_5$ ($803.54 \text{ g mol}^{-1}$): C 64.17, H 9.89, N 8.70; found: C 63.01, H 9.89, N 8.57%. (Remark: the elemental analysis is calculated by assuming the formation of $[^nBu_4N]_2[Ni(opooMe)]$ (**6**) in pure state. The observed values do not deviate severely from calculated ones, indicating that the measurement of the elemental analysis of the obtained orange powder alone is not suited to decide whether pure **8** is formed or not.)

The orange powder was dissolved in MeCN, acetone and DMF, respectively, and the solutions obtained were subjected to diffusion controlled crystallizations against Et_2O . In all three cases the whole amount of the orange powder did crystallize, as finally colourless solvent mixtures were obtained. Furthermore, in all three cases one kind of crystal in minority has been obtained. Unit cell measurements by single-crystal X-ray diffraction studies revealed the crystals formed in minority to be identical. A full characterization in one selected case did prove the formation of $[^nBu_4N]_2[Ni(opba)]$ (**5**). Thus, independent of the solvent used to dissolve the orange coloured powder for crystallization, **5** is always formed in pure state. The second kind of crystal formed in majority has been subjected to analogous X-ray studies as well. These studies did reveal these crystals to be $[^nBu_4N]_2[Ni(opooMe)]$ (**6**), as reported earlier.¹³ No further characterization of **5** and **6** has been performed, as the identities of both Ni^{II} complexes are established unambiguously by the X-ray studies.

Cu^{II} COMPLEXES. The previous procedure was employed to synthesize the Cu^{II} complexes with $[Cu_2(OAc)_4(H_2O)_2]$ (0.27 g, 0.0007 mol), the recrystallized material (0.41 g, 0.0014 mol) and $[^nBu_4N]OH$ (3.62 g, 0.0056 mol). The solid material obtained after precipitation was purple coloured. Anal. calcd (%) for $C_{43}H_{79}CuN_5O_5$ ($809.77 \text{ g mol}^{-1}$): C 63.79, H 9.83, N 8.65; found: C 63.04, H 9.80, N 8.43%. (Remark: the elemental analysis is calculated by assuming the formation of $[^nBu_4N]_2[Cu(opooMe)]$ (**8**) in pure state. The observed values do not deviate severely from calculated ones, indicating that the measurement of the elemental analysis of the obtained purple powder is not suited to guarantee the formation of a pure complex.) As described for the Ni^{II} complexes, the purple powder was subjected to different crystallizations. Similarly in all three cases two different kinds of crystals in minority ($[^nBu_4N]_2[Cu(opba)]$, **7**) and majority ($[^nBu_4N]_2[Cu(opooMe)]$, **8**) were formed, as analyzed by X-ray studies as described before.

COCRYSTALLIZATION OF THE ORANGE AND PURPLE POWDERS. A mixture of the orange powder (99 mg) and the purple powder (1 mg) was dissolved in MeCN and the resulting solution was subjected to diffusion controlled crystallization against Et_2O . Large, orange coloured crystals were formed in minority possessing well shaped faces (Fig. S16†). The crystals formed in minority were subjected to EPR measurements, establishing the formation of **7**@**5**. The results obtained from these measurements agree completely with already reported ones.¹⁵ The crystals formed in majority were subjected to EPR measurements as well, establishing the formation of **8**@**6**. The results obtained from these measurements agree completely with that in our recent report.¹³

Resolution process of the material obtained from the reaction of opbaH₂Et₂ with MeNH₂ into its components

The reaction of opbaH₂Et₂ with MeNH₂ in MeOH has been repeated as described before, giving identical analytical results. Solvent extraction was carried out in a standard Soxhlet apparatus of 250 mL volume, using THF, MeOH and EtOH as solvents, successively.

EXTRACTION WITH THF. The Soxhlet thimble was charged with 2 g of finely ground crude, and extracted first with 100 mL of THF for three hours. The solvent was removed using a rotary evaporator and the solid material obtained dried *in vacuo*. Crop **A** (opbaH₂Me₂, **2**): yield: 0.13 g (6%), based on the used crude. Anal. calcd (%) for $C_{12}H_{12}N_2O_6$ ($280.23 \text{ g mol}^{-1}$): C 51.43, H 4.32, N 10.00; found: C 51.40, H 4.19, N 9.91. IR: $\nu = 3345(s)$, 3236(b) (NH); 1717(s), 1682(s), 1600(s) (CO). 1H NMR: $\delta = 3.87$ (s, 6H, $H^{1,1'}$), 7.31 (dd, 2H, $H^{6,6'}$), 7.57 (dd, 2H, $H^{5,5'}$), 10.40 (s, 2H, NH). $^{13}C\{^1H\}$ NMR: $\delta = 53.2$ ($C^{1,1'}$), 125.6 ($C^{6,6'}$), 126.3 ($C^{5,5'}$), 129.6 ($C^{4,4'}$), 155.3 ($C^{3,3'}$), 160.7 ($C^{2,2'}$). The IR, 1H and ^{13}C NMR spectra of **2** are given in Fig. S3 and S4,† respectively.

The prevailed residue in the Soxhlet thimble after THF extraction (**B**) was dried by a stream of argon. The 1H and ^{13}C NMR spectra of residue **B** are given in the ESI in Fig. S5.†

EXTRACTION WITH MeOH. After drying **B**, this residue was extracted with 100 mL of MeOH for 7 hours to leave insoluble off-white material in the Soxhlet thimble, referred to as residue **D**. The solid **D** was collected and recrystallized from MeOH:DMSO (2:1) and dried *in vacuo*. According to the analytical data given below, **D** refers to exclusively 1,4-dihydro-2,3-quinoxalinedione (**3**): yield: 0.06 g (3%), based on the used crude. Anal. calcd (%) for $C_8H_6N_2O_2$ ($162.15 \text{ g mol}^{-1}$): C 59.26, H 3.73, N 17.28; found: C 59.28, H 3.70, N 17.24%. IR: $\nu = 3023$ (m) (NH); 2865(m), 2833(m) (CH); 1655(s), 1605(m) (CO). 1H NMR: $\delta = 7.09$ (dd, 2H, $H^{1,1'}$), 7.12 (dd, 2H, $H^{2,2'}$), 11.90 (s, 2H, NH). $^{13}C\{^1H\}$ NMR: $\delta = 115.0$ ($C^{1,1'}$), 122.9 ($C^{2,2'}$), 125.5 ($C^{3,3'}$), 155.1 ($C^{4,4'}$). The IR, 1H and ^{13}C NMR spectra of **3** are given in Fig. S6 and S7,† respectively.

The MeOH extract (**C**) was evaporated to dryness. The 1H and ^{13}C NMR spectra of **C** are given in Fig. S8.† According to its NMR characterization, **C** was found to be composed of at least two different compounds. Therefore, **C** was subjected to a further Soxhlet extraction.

EXTRACTION WITH EtOH. **C** was placed in a Soxhlet extractor again and extracted with 100 mL of EtOH for 10 hours. The EtOH insoluble material **F** was collected and dried *in vacuo*. According to the analytical data given below, **F** refers exclusively to *o*-phenylenebis(*N'*-methyloxamide) (opboH₄Me₂, **4**): yield: 0.02 g (1%), based on the used crude. Anal. calcd (%) for $C_{12}H_{14}N_4O_4$ ($278.26 \text{ g mol}^{-1}$): C 51.80, H 5.07, N 20.14; found: C 51.81, H 5.02, N 20.09. IR: $\nu = 3378(s)$, 3318(s), 3258(sh) (NH); 1705(m), 1681(s), 1655(s), 1601(s) (CO). 1H NMR: $\delta = 2.74$ (d, 6H, $H^{1,1'}$), 7.30 (dd, 2H, $H^{6,6'}$), 7.60 (dd, 2H, $H^{5,5'}$), 8.96 (q, 2H, $NHCH_3$), 10.47 (s, 2H, $NHAr$). $^{13}C\{^1H\}$ NMR: $\delta = 26.0$ ($C^{1,1'}$), 125.3 ($C^{6,6'}$), 126.0 ($C^{5,5'}$), 129.8 ($C^{4,4'}$), 158.6 ($C^{2,2'}$), 160.0 ($C^{3,3'}$). The IR, 1H and ^{13}C NMR spectra of **4** are given in Fig. S9 and S10,† respectively.

The EtOH extract **E** was evaporated in a rotary evaporator and the white solid obtained was collected and dried *in vacuo*. According to the analytical data given below, **E** refers exclusively to methyl ester of *o*-phenylene(*N'*-methyloxamide) (oxamic acid) (opooH₃Me₂, **1**): yield: 1.78 g (89%), based on the used crude. Anal. calcd (%) for C₁₂H₁₃N₃O₅ (279.25 g mol⁻¹): C 51.61, H 4.69, N 15.05; found: C 51.56, H 4.63, N 14.99. IR: ν = 3303(sh), 3254(m) (NH); 1732(m), 1709(s), 1654(s), 1597(s), (CO). ¹H NMR: δ = 2.74 (d, 3H, H¹²), 3.87 (s, 3H, H¹), 7.30 (m, 2H, H^{6,7}), 7.54 (dd, 1H, H⁸), 7.66 (dd, 1H, H⁵), 8.96 (m, 1H, NHC¹²), 10.33 (s, 1H, NHC⁹), 10.57 (s, 1H, NHC⁴). ¹³C{¹H} NMR: δ = 26.0 (C¹²), 53.3 (C¹), 125.0 (C⁷), 125.8 (C⁶), 125.9 (C⁸), 126.4 (C⁵), 129.1 (C⁹), 130.2 (C⁴), 155.2 (C¹¹), 158.5 (C¹⁰), 160.0 (C³), 160.2 (C²). The IR, ¹H and ¹³C NMR spectra of **1** are given in Fig. S11 and S12,[†] respectively.

Synthesis of the ethyl ester of *o*-phenylene(*N'*-methyloxamide)- (oxamic acid) (opooH₃EtMe, **9**)

According to the literature,¹³ a solution of opbaH₂Et₂ (0.006 mole, 1.84 g) in absolute EtOH (50 mL) was treated with MeNH₂ (0.15 g, 0.005 mole, 33% in EtOH) under continuous vigorous stirring at 25 °C. After stirring for 30 minutes, the white precipitate obtained was filtered off, washed with EtOH and Et₂O, and dried *in vacuo*. Yield: 0.91 g (52%). Anal. calcd (%) for C₁₃H₁₅N₃O₅ (293.28 g mol⁻¹): C 53.24, H 5.16, N 14.33; found: C 53.45, H 5.20, N 14.91. IR: ν = 3308(m), 3257(m) (NH); 1732(sh), 1711(s), 1655(s), 1595(s), (CO). ¹H NMR: δ = 1.33 (t, 3H, H¹), 2.75 (d, 3H, H¹³), 4.32 (q, 2H, H²), 7.30 (m, 2H, H^{7,8}), 7.55 (dd, 1H, H⁹), 7.67 (dd, 1H, H⁶), 8.96 (m, 1H, NHC¹³), 10.35 (s, 1H, NHC¹⁰) and 10.52 (s, 1H, NHC⁵). ¹³C{¹H} NMR: δ = 13.7 (C¹), 26.0 (C¹³), 62.6 (C²), 125.0 (C⁸), 125.8 (C⁷), 125.9 (C⁹), 126.4 (C⁶), 129.2 (C¹⁰), 130.1 (C⁵), 155.4 (C¹²), 158.5 (C¹¹), 160.0 (C⁴), 160.2 (C³).

The IR, ¹H and ¹³C NMR spectra of **9** are given in Fig. S13 and S14,[†] respectively.

X-ray crystallography

Intensity data for **1**, 2·2DMSO, **5** and **7**, respectively, were collected on an Oxford Gemini S diffractometer with Mo K α radiation (2·2DMSO) or Cu K α radiation (**1**, **5** and **7**). The structures were solved by direct methods and refined by full-matrix least-squares methods on *F*² with the SHELXTL-97 program package.²⁴ All non-hydrogen atoms were refined anisotropically. All C-bonded hydrogen atoms were geometrically placed and refined isotropically in riding modes using default SHELXTL parameters. The positions of N-bonded hydrogen atoms were taken from difference Fourier maps and refined isotropically. CCDC numbers 888732 (**1**), 888733 (2·2DMSO), 888734 (**5**) and 888735 (**7**).

Conclusion

It could be shown that the use of MeOH as a solvent for the amide formation reaction of opbaH₂Et₂ with sub-stoichiometric amounts of MeNH₂ is not suited to guarantee the

formation of solely the methyl ester opooH₃Me₂, **1**. This observation could be generalized in the sense that for amide formations of bis(oxamic acid) esters with primary alkylamines the use of MeOH should be avoided. Instead, absolute EtOH as a solvent should be applied, as shown for the formation of the ethyl ester opooH₃EtMe, **9**. Moreover, the observed formation of **1** together with those of opbaH₂Me₂ (**2**) by reacting opbaH₂Et₂ with MeNH₂ in MeOH may give stimulation for the research of amine catalyzed related transesterification reactions.

The observation that from dissolved mixtures of the complexes **5**–**8** single crystals of **7**@**5** together with single crystals of **8**@**6** are formed is a nice example for the supramolecular recognition of structurally related complexes.

Acknowledgements

This work has been supported by the Deutsche Forschungsgemeinschaft through project FOR 1154 "Towards Molecular Spintronics". M. A. A. thanks the DAAD for a scholarship.

Notes and references

- 1 E. Pardo, R. Ruiz, J. Cano, X. Ottenwaelder, R. Lescouezec, Y. Journaux, F. Lloret and M. Julve, *Dalton Trans.*, 2008, 2780.
- 2 W. Gaade, *Recl. Trav. Chim. Pays-Bas*, 1936, **55**, 324.
- 3 Y. Pei, O. Kahn and J. Sletten, *J. Am. Chem. Soc.*, 1986, **108**, 3143.
- 4 H. Stumpf, Y. Pei, O. Kahn, J. Sletten and J. Renard, *J. Am. Chem. Soc.*, 1993, **115**, 6738.
- 5 C. Paul-Roth, *C. R. Chim.*, 2005, **8**, 1232.
- 6 T. Rüffer, B. Bräuer, F. Meva, B. Walfort, G. Salvan, A. Powell, I. Hewitt, L. Sorace and A. Caneschi, *Inorg. Chim. Acta*, 2007, **360**, 3777.
- 7 T. Rüffer, B. Bräuer, A. Powell, I. Hewitt and G. Salvan, *Inorg. Chim. Acta*, 2007, **360**, 3475.
- 8 T. Rüffer, B. Bräuer, F. Meva and B. Walfort, *J. Chem. Soc., Dalton Trans.*, 2008, 5089.
- 9 T. Rüffer and B. Bräuer, *Anal. Sci.: X-Ray Struct. Anal. Online*, 2007, **23**, x53.
- 10 B. Cervera, J. L. Sanz, M. J. Ibanez, G. Vila, F. Lloret, M. Julve, R. Ruiz, X. Ottenwaelder, A. Aukauloo, S. Poussereau, Y. Journaux and M. C. Munoz, *J. Chem. Soc., Dalton Trans.*, 1998, 781.
- 11 (a) R. Ruiz, C. Barland, A. Aukauloo, E. Mallart, Y. Journaux, J. Cano and M. Muñoz, *J. Chem. Soc., Dalton Trans.*, 1997, 745; (b) X. Ottenwaelder, A. Aukauloo, Y. Journaux, R. Carrasco, J. Cano, B. Cervera, I. Castro, S. Curreli, M. Munoz, A. Rosello, B. Soto and R. Ruiz, *Dalton Trans.*, 2005, 2516; (c) I. Fernandez, J. Pedro, A. Rosello, R. Ruiz, I. Castro, X. Ottenwaelder and Y. Journaux, *Eur. J. Org. Chem.*, 2001, 1235.

- 12 R. Ruiz, C. Barland, Y. Journaux and J. Colin, *Chem. Mater.*, 1997, **9**, 201.
- 13 M. A. Abdulmalic, A. Aliabadi, A. Petr, Y. Krupskaya, V. Kataev, B. Büchner, T. Hahn, J. Kortus and T. Rüffer, *Dalton Trans.*, 2012, DOI: 10.1039/C2DT31802D.
- 14 For an optical photograph of the two different kinds of single crystals see Fig. S16.†
- 15 B. Bräuer, F. Weigend, M. Fittipaldi, D. Gatteschi, E. J. Reijerse, A. Guerri, S. Ciattini, G. Salvan and T. Rüffer, *Inorg. Chem.*, 2008, **47**, 6633.
- 16 H. D. Flack, *Acta Crystallogr., Sect. A: Fundam. Crystallogr.*, 1983, **39**, 876.
- 17 S. Martin, J. I. Beitia, M. Ugalde, P. Vitoria and R. Cortes, *Acta Crystallogr., E*, 2002, **58**, o913.
- 18 E. Q. Gao, D. Z. Liao, Z. H. Jiang and S. P. Yan, *Acta Crystallogr., Sect. C: Cryst. Struct. Commun.*, 2001, **57**, 807.
- 19 E. Q. Gao, *Acta Crystallogr. E*, 2004, **60**, m1700.
- 20 B. Cervera, J. L. Sanz, M. J. Ibanez, G. Vila, F. Lloret, M. Julve, R. Ruiz, X. Ottenwaelder, A. Aukauloo, S. Poussereau, Y. Journaux and M. C. Munoz, *J. Chem. Soc., Dalton Trans.*, 1998, 781.
- 21 S. S. Turner, C. Michaut, O. Kahn, L. Quahab, A. Lecas and E. Amouyal, *New J. Chem.*, 1995, **19**, 773.
- 22 R. D. Shannon, *Acta Crystallogr., Sect. A: Cryst. Phys., Diffraction, Theor. Gen. Cryst.*, 1976, **32**, 751.
- 23 D. D. Perrin and W. L. F. Armarego, *Purification of Laboratory Chemicals*, Pergamon, New York, 1988, 3rd edn.
- 24 (a) G. M. Sheldrick, *SHELXS-97, Program for Crystal Structure Solution*, University of Göttingen, Göttingen, Germany, 1997; (b) G. M. Sheldrick, *SHELXL-97, Program for Crystal Structure Refinement*, University of Göttingen, Germany, 1997, Release 97-2.